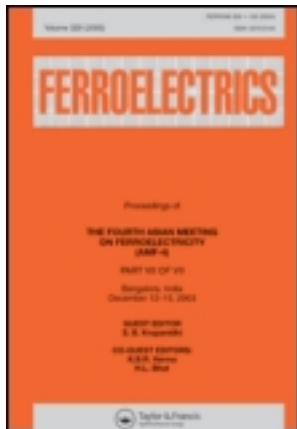


This article was downloaded by: [Institute of Mechanics]

On: 22 March 2012, At: 20:37

Publisher: Taylor & Francis

Informa Ltd Registered in England and Wales Registered Number: 1072954 Registered office: Mortimer House, 37-41 Mortimer Street, London W1T 3JH, UK



## Ferroelectrics

Publication details, including instructions for authors and subscription information:

<http://www.tandfonline.com/loi/gfer20>

### Synthesis and Characterization of (1-x)(Na<sub>0.5</sub>Bi<sub>0.5</sub>)TiO<sub>3</sub>-xAl<sub>6</sub>Bi<sub>2</sub>O<sub>12</sub> Solid Solution

Y. Zhen<sup>a</sup>, S. Hall<sup>a</sup>, T. Brown<sup>a</sup>, E. C. Ekuma<sup>a</sup>, Z. Bell<sup>a</sup>, Z. W. Sun<sup>b</sup> & J. T. Wang<sup>a</sup>

<sup>a</sup> Department of Physics, Southern University and A&M College Baton Rouge, LA, 70813, USA

<sup>b</sup> Institute of Mechanics, Chinese Academy of Sciences, 100190, Beijing, People's Republic of China

Available online: 30 Jun 2011

To cite this article: Y. Zhen, S. Hall, T. Brown, E. C. Ekuma, Z. Bell, Z. W. Sun & J. T. Wang (2011): Synthesis and Characterization of (1-x)(Na<sub>0.5</sub>Bi<sub>0.5</sub>)TiO<sub>3</sub>-xAl<sub>6</sub>Bi<sub>2</sub>O<sub>12</sub> Solid Solution, *Ferroelectrics*, 413:1, 192-205

To link to this article: <http://dx.doi.org/10.1080/00150193.2011.554147>

PLEASE SCROLL DOWN FOR ARTICLE

Full terms and conditions of use: <http://www.tandfonline.com/page/terms-and-conditions>

This article may be used for research, teaching, and private study purposes. Any substantial or systematic reproduction, redistribution, reselling, loan, sub-licensing, systematic supply, or distribution in any form to anyone is expressly forbidden.

The publisher does not give any warranty express or implied or make any representation that the contents will be complete or accurate or up to date. The accuracy of any instructions, formulae, and drug doses should be independently verified with primary sources. The publisher shall not be liable for any loss, actions, claims, proceedings, demand, or costs or damages whatsoever or howsoever caused arising directly or indirectly in connection with or arising out of the use of this material.

# Synthesis and Characterization of (1-x)(Na<sub>0.5</sub>Bi<sub>0.5</sub>)TiO<sub>3</sub>-xAl<sub>6</sub>Bi<sub>2</sub>O<sub>12</sub> Solid Solution

Y. ZHEN,<sup>1</sup> S. HALL,<sup>1</sup> T. BROWN,<sup>1</sup> E. C. EKUMA,<sup>1</sup>  
Z. BELL,<sup>1</sup> Z. W. SUN,<sup>2</sup> AND J. T. WANG<sup>1,\*</sup>

<sup>1</sup>Department of Physics, Southern University and A&M College  
Baton Rouge, LA 70813, USA

<sup>2</sup>Institute of Mechanics, Chinese Academy of Sciences, 100190 Beijing,  
People's Republic of China

*The new lead-free (1-x)(Na<sub>0.5</sub>Bi<sub>0.5</sub>)TiO<sub>3</sub>-xAl<sub>6</sub>Bi<sub>2</sub>O<sub>12</sub> compounds with x = 0.01, 0.02, and 0.03 have been synthesized by conventional solid-state ceramic-fabrication technique. Systematic investigations on the dielectric, ferroelectric and piezoelectric properties of both poled and unpoled samples have been carried out. It was revealed that the dielectric and piezoelectric properties are improved by the addition of an appropriate amount of Al<sub>6</sub>Bi<sub>2</sub>O<sub>12</sub>. Comparisons of these properties between poled and unpoled samples are presented. It is found that Curie temperatures and remnant polarization are increased after poling. The coercive field is, however, decreased after poling.*

**Keywords** (1-x)(Na<sub>0.5</sub>Bi<sub>0.5</sub>)TiO<sub>3</sub>-xAl<sub>6</sub>Bi<sub>2</sub>O<sub>12</sub> solid solution; dielectric; ferroelectric; piezoelectric

DOI: 10.1063/1.2967335

## 1. Introduction

Due to its excellent ferroelectric properties, Lead zirconium titanate (PZT) ceramics with distorted perovskite structure have been widely used in devices such as transducers, sensors, and actuators [1, 2]. However, the toxicity of lead in PZT raises a serious environmental concern. Therefore, it is essential to seek environment-respectfully ferroelectric ceramics which maintain high performance of ferroelectric behaviors comparable or superior to PZT. Non-lead ferroelectric material becomes more and more desirable. Many studies on these type of lead-free ferroelectric materials have widely been made [3–11]. In recent years, experimental studies on (Na<sub>0.5</sub>Bi<sub>0.5</sub>)TiO<sub>3</sub> (NBT) have been performed extensively. NBT is rhombohedral perovskite lead-free ferroelectrics below about 200°C. It will transform from ferroelectric phase to anti-ferroelectric phase at about this temperature point. When the temperature is increased to 320°C, NBT goes into paraelectric phase. Because of its large remnant polarization ( $P_r = 38 \mu\text{C}/\text{cm}^2$ ), NBT is a promising lead-free piezoelectric ceramic. However, its high coercive field ( $E_c = 73 \text{ kV}/\text{cm}$ ) and high conductivity limit its applications. Many efforts have been made in order to improve the performance of NBT by forming NBT-based solid solutions [12–16].

---

Received in final form October 26, 2010.

\*Corresponding author. E-mail: wangjintong@gmail.com

Theoretical studies predict that materials with general formula  $\text{BiMO}_3$  (M is transition metals) are capable to exhibit high ferroelectricity and magnetism. A large ferroelectric polarization was reported [17] in thin films of  $\text{BiFeO}_3$ . Among these materials, bismuth aluminate  $\text{BiAlO}_3$  (BAO) and bismuth gallium  $\text{BiGaO}_3$  (BGO) have been predicted to be promising candidates for lead-free ferroelectric materials because of their large ferroelectric polarization and piezoelectricity by theoretical calculations [18]. However,  $\text{BiMO}_3$  have to be prepared at high pressure and high temperature conditions except  $\text{BiFeO}_3$  [19]. Therefore, many studies have been made in which  $\text{BiMO}_3$  have been used as an addition to improve the performance of NBT in the form of solid solution. Experimental studies of NBT- $\text{BiMO}_3$  (NBT-BM) have been carried out. The results implied that NBT-BM could be excellent lead-free candidates for ferroelectric material. The solid solution is a ceramics with polar rhombohedral symmetry and it has a Curie temperature ( $T_C$ ) around 270–310°C [20, 21]. Yu *et al.* have synthesized and studied NBT- $\text{BiAlO}_3$  solid solution [20]. In this paper, using  $\text{Al}_6\text{Bi}_2\text{O}_{12}$  as one of starting materials, new solid solution NBT- $\text{Al}_6\text{Bi}_2\text{O}_{12}$  is synthesized by conventional solid-state reaction method which has a slightly different process from Yu *et al.*'s work [20]. The temperature dependence of dielectric constants of the solid solutions have been measured and the polarization-electric field hysteresis behaviors and the piezoelectric properties have been investigated at room temperature for poled and unpoled samples, respectively.

## 2. Experimental

Reagent-grade  $\text{Na}_2\text{CO}_3$ ,  $\text{Bi}_2\text{O}_3$ , and  $\text{TiO}_2$  compositions were used to form the precursor  $(\text{Na}_{0.5}\text{Bi}_{0.5})\text{TiO}_3$  (NBT). They are first mixed stoichiometrically according to the formula,  $(\text{Na}_{0.5}\text{Bi}_{0.5})\text{TiO}_3$  and ball-milled. The mixture was calcined at 800°C and the NBT is formed. The NBT powder and  $\text{Al}_6\text{Bi}_2\text{O}_{12}$  powder were then mixed stoichiometrically according to the compositional formula  $(1-x)(\text{Na}_{0.5}\text{Bi}_{0.5})\text{TiO}_3\text{-}x\text{Al}_6\text{Bi}_2\text{O}_{12}$  with  $x = 0.01, 0.02, 0.03$  and ball-milled with polyvinyl alcohol as a binder for 4h. Then, the compositions were pressed into pellets of 10mm in diameter and 0.5–0.6mm in thickness using a hydraulic press. The pelletized samples were placed in a sealed crucible and finally sintered at 1100°C for 12h in a programmable furnace. This preparation procedure is slightly different from the one adopted in the reference work [20] and the present method was still to obtain the perovskite phase. The powders were characterized by X-ray diffraction (XRD) using Rigaku x-ray diffractometer with  $\text{Cu K}\alpha$  radiation source for crystal structure analysis. The sintered pellets were polished and silver paste was applied to the surfaces of the pellets as the electrodes. The samples were poled in a silicone oil bath at 80°C by applying dc electric field of 50kV/cm for 30 min. The dielectric constant and loss for poled and unpoled samples were measured using a HP Model 4284A LCR meter at the temperature range from 40°C to 600°C in the frequency range from 100 Hz to 1 MHz. Polarizations versus applied electric field (hysteresis) measurements for poled and unpoled samples were performed with a Radiant RT66 at room temperature. The Piezoelectric properties of the poled and unpoled samples were measured using a ZYGO laser interferometer.

## 3. Results and Discussion

Figure 1 shows the XRD patterns of  $(1-x)(\text{Na}_{0.5}\text{Bi}_{0.5})\text{TiO}_3\text{-}x\text{Al}_6\text{Bi}_2\text{O}_{12}$  with  $x = 0.02$ . The XRD patterns reveal that all  $(1-x)(\text{Na}_{0.5}\text{Bi}_{0.5})\text{TiO}_3\text{-}x\text{Al}_6\text{Bi}_2\text{O}_{12}$  with  $x = 0.01, 0.02, 0.03$  have a rhombohedral perovskite structure. It can also be seen that a small peak at

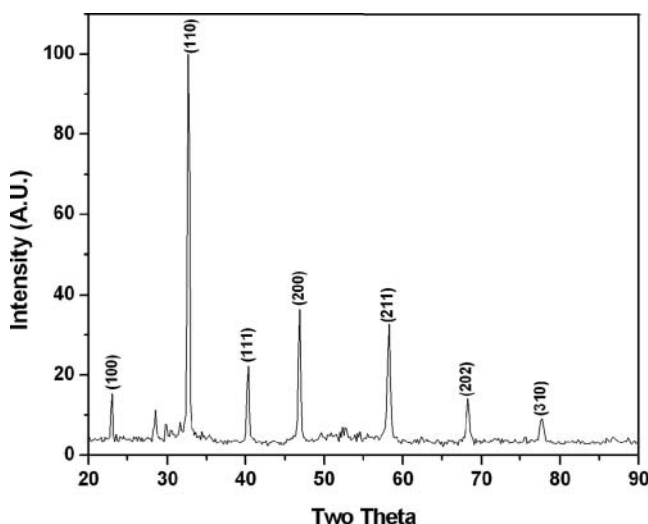


**Figure 1.** XRD pattern of the  $(1-x)(\text{Na}_{0.5}\text{Bi}_{0.5})\text{TiO}_3-x\text{Al}_6\text{Bi}_2\text{O}_{12}$  solid solution ( $x = 0.02$ ) at room temperature.

Two theta equal to roughly  $28^\circ$ . This indicates the existence of an impurity phase possibly due to the formation of a small amount of bismuth-deficient  $\text{Bi}_2\text{Al}_4\text{O}_9$ -type secondary phases. Approximately, the impurity is 5%. This impurity can also be observed in Bismuth Aluminate prepared using a high pressure method [19].

The temperature dependences of the dielectric constant of  $(1-x)(\text{Na}_{0.5}\text{Bi}_{0.5})\text{TiO}_3-x\text{Al}_6\text{Bi}_2\text{O}_{12}$  for unpoled and poled samples at 100Hz are shown in Figs. 2 and 3 respectively. Figs. 4 and 5 show that transition temperature and peak values of the dielectric constants of  $(1-x)(\text{Na}_{0.5}\text{Bi}_{0.5})\text{TiO}_3-x\text{Al}_6\text{Bi}_2\text{O}_{12}$  versus the different concentration of  $\text{Al}_6\text{Bi}_2\text{O}_{12}$   $x$  for unpoled and poled samples, respectively. From Fig. 2, it can be seen that broadness of the dielectric peak increases with increasing  $x$  for unpoled sample. It may indicate that the concentration rate  $x$  may affect the type of ferroelectric transition from regular one

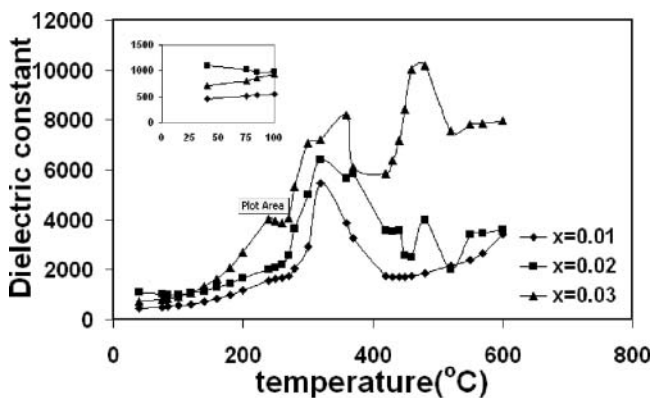


**Figure 2.** Temperature-dependence of the dielectric constant of  $(1-x)(\text{Na}_{0.5}\text{Bi}_{0.5})\text{TiO}_3-x\text{Al}_6\text{Bi}_2\text{O}_{12}$  ( $x = 0.01, 0.02, \text{ and } 0.03$ ) at 100 Hz before poling (lines for guiding the eyes only).

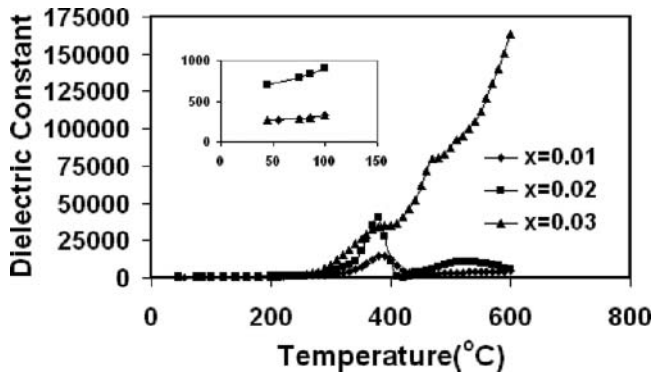


**Figure 3.** Temperature-dependence of the dielectric constant of  $(1-x)(\text{Na}_{0.5}\text{Bi}_{0.5})\text{TiO}_3-x\text{Al}_6\text{Bi}_2\text{O}_{12}$  ( $x = 0.01, 0.02,$  and  $0.03$ ) at 100 Hz after poling (lines for guiding the eyes only).

to relaxor. And there are two dielectric peaks for unpoled sample with  $x = 0.03$ . It may imply that there are two phase transitions, i.e. from ferroelectric to antiferroelectric at about  $350^\circ\text{C}$  and from antiferroelectric to paraelectric at about  $500^\circ\text{C}$  in this unpoled sample ( $x = 0.03$ ). From Fig. 3, it can be seen that dielectric constant increases through entirely measurement temperature range at 100Hz for poled sample with  $x = 0.03$ . Transition temperature might correspond to the decomposition temperature of rhombohedral phase. It implies that transition from ferroelectric phase to antiferroelectric phase isn't completed before  $400^\circ\text{C}$ . It may indicate that poling can enlarge the ferroelectric temperature region, that is, increase the ferroelectric phase transition temperature. It can, in turn, significantly enhance the application potential. From Figs. 2, and 3, we see that the dielectric constant

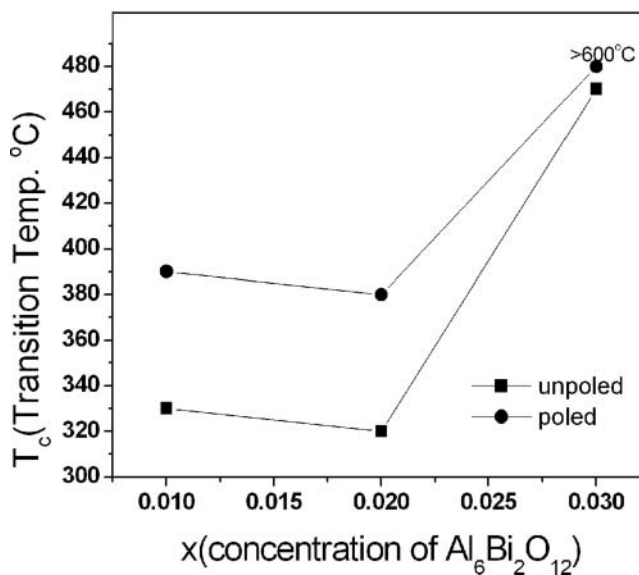


**Figure 4.** concentration  $x$ -dependence of transition temperature  $T_c$  of  $(1-x)(\text{Na}_{0.5}\text{Bi}_{0.5})\text{TiO}_3-x\text{Al}_6\text{Bi}_2\text{O}_{12}$  at 100 Hz (lines for guiding the eyes only).

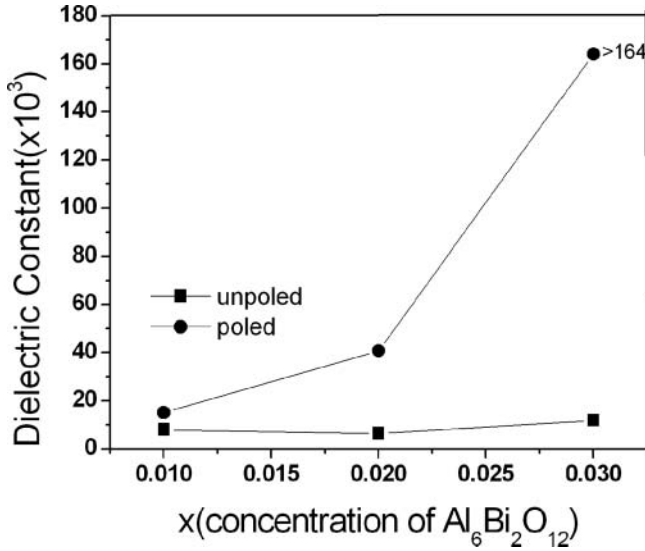


**Figure 5.** Concentration  $x$ -dependence of maximum dielectric constant of  $(1-x)(\text{Na}_{0.5}\text{Bi}_{0.5})\text{TiO}_3-x\text{Al}_6\text{Bi}_2\text{O}_{12}$  at 100 Hz (lines for guiding the eyes only).

peak at 100Hz for pole sample with  $x = 0.01$  is broader than the one for unpoled sample. However, we have yet no interpretation for this finding. It also found that  $T_c$  slightly shifts to lower temperature and the peak values of dielectric constant around  $320^\circ\text{C}$ – $400^\circ\text{C}$  at 100 Hz increase with increasing  $x$  shown in Figs. 4 and 5.

Figures 6 and 7 show the temperature-dependence of the dielectric response of  $(1-x)(\text{Na}_{0.5}\text{Bi}_{0.5})\text{TiO}_3-x\text{Al}_6\text{Bi}_2\text{O}_{12}$  ( $x = 0.01$ ) at various frequencies in the temperature range from  $45^\circ\text{C}$ – $600^\circ\text{C}$  for unpoled and poled samples, respectively. The dielectric constants have a well-defined maximum around  $350^\circ\text{C}$  for poled samples. The dielectric constant peaks increase and shift to a higher temperature for poled sample compared with these

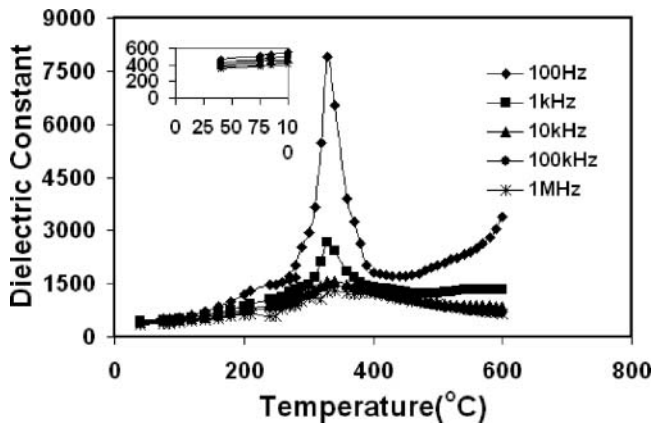


**Figure 6.** Temperature-dependence of the dielectric constant of  $(1-x)(\text{Na}_{0.5}\text{Bi}_{0.5})\text{TiO}_3-x\text{Al}_6\text{Bi}_2\text{O}_{12}$  ( $x = 0.01$ ) before poling (lines for guiding the eyes only).

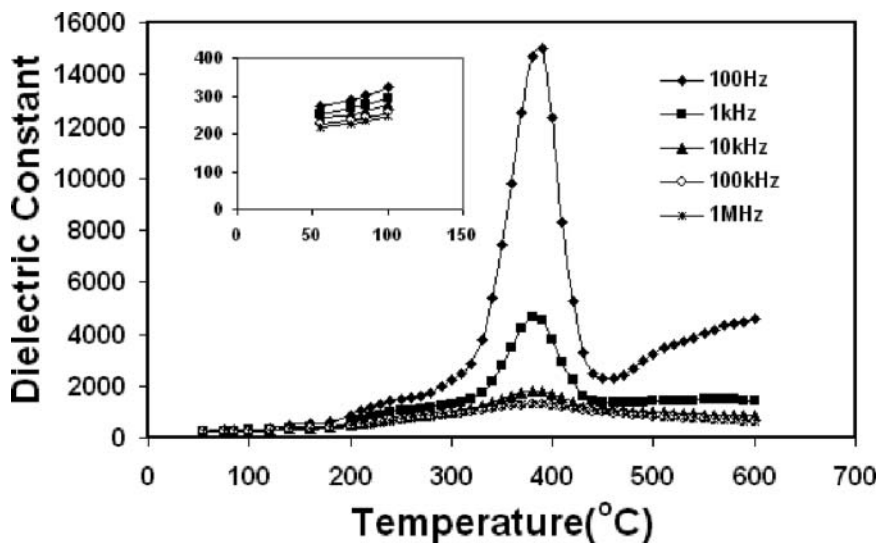


**Figure 7.** Temperature-dependence of the dielectric constant of  $(1-x)(\text{Na}_{0.5}\text{Bi}_{0.5})\text{TiO}_3-x\text{Al}_6\text{Bi}_2\text{O}_{12}$  ( $x = 0.01$ ) after poling (lines for guiding the eyes only).

for unpoled sample (around  $325^\circ\text{C}$ ). Furthermore, the dielectric constants decrease with increasing frequencies over the entire range of temperature employed.

Figures 8 and 9 show the temperature dependence of the dielectric loss of  $(1-x)(\text{Na}_{0.5}\text{Bi}_{0.5})\text{TiO}_3-x\text{Al}_6\text{Bi}_2\text{O}_{12}$  ( $x = 0.01, 0.02$  and  $0.03$ ) for unpoled and poled samples,

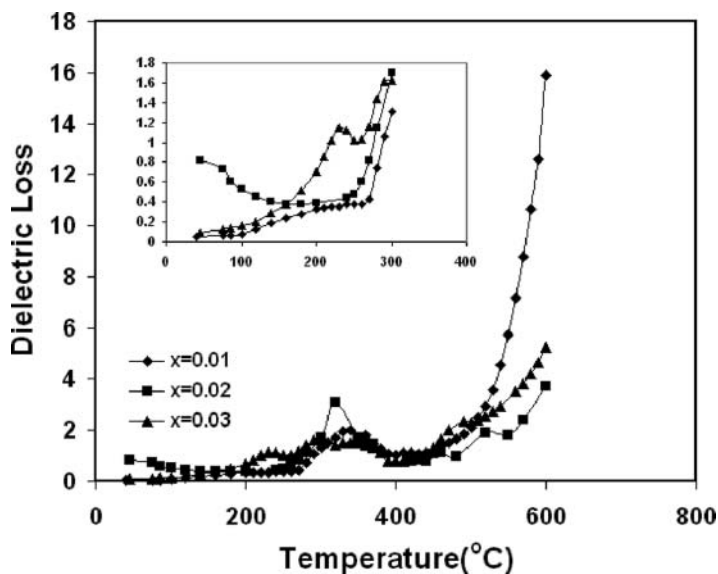


**Figure 8.** Temperature-dependence of the dielectric loss of  $(1-x)(\text{Na}_{0.5}\text{Bi}_{0.5})\text{TiO}_3-x\text{Al}_6\text{Bi}_2\text{O}_{12}$  ( $x = 0.01, 0.02$ , and  $0.03$ ) at 100 Hz before poling (lines for guiding the eyes only).

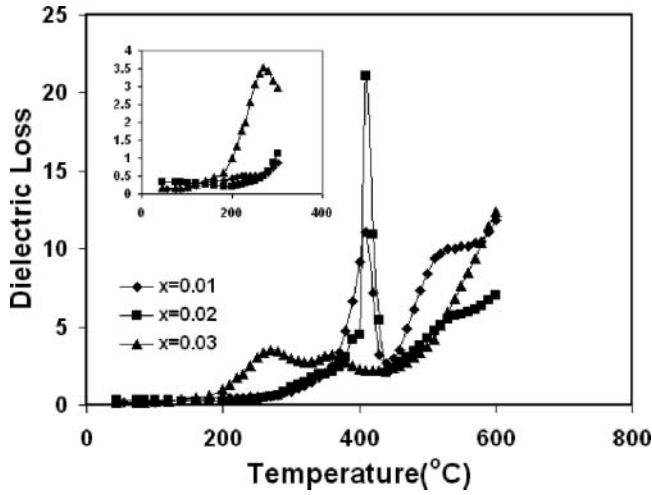


**Figure 9.** Temperature-dependence of the dielectric loss of  $(1-x)(\text{Na}_{0.5}\text{Bi}_{0.5})\text{TiO}_3-x\text{Al}_6\text{Bi}_2\text{O}_{12}$  ( $x = 0.01, 0.02,$  and  $0.03$ ) at 100 Hz after poling (lines for guiding the eyes only).

respectively. Fig. 10 shows concentration of  $\text{Al}_6\text{Bi}_2\text{O}_{12}$   $x$ -dependence of dielectric loss at  $75^\circ\text{C}$  and 100Hz. At higher temperature above  $500^\circ\text{C}$  for unpoled sample it can be seen in Fig. 8 that increasing the content of  $\text{Al}_6\text{Bi}_2\text{O}_{12}$  will lower the dielectric loss and it indicates that the addition of  $\text{Al}_6\text{Bi}_2\text{O}_{12}$  provides an effective barrier to suppress the movement of mobile ions in  $(\text{Na}_{0.5}\text{Bi}_{0.5})\text{TiO}_3$  for unpoled samples [23, 24]. For poled samples in Fig. 9,

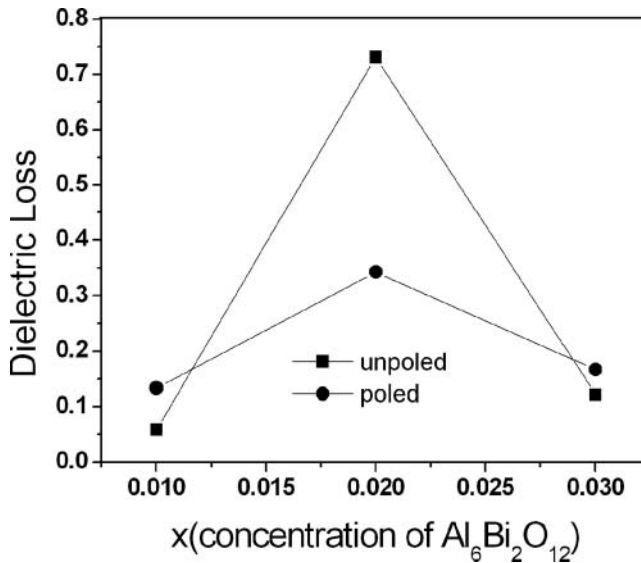


**Figure 10.** Concentration  $x$ -dependence of dielectric loss of  $(1-x)(\text{Na}_{0.5}\text{Bi}_{0.5})\text{TiO}_3-x\text{Al}_6\text{Bi}_2\text{O}_{12}$  At  $75^\circ\text{C}$  and 100 Hz (lines for guiding the eyes only).



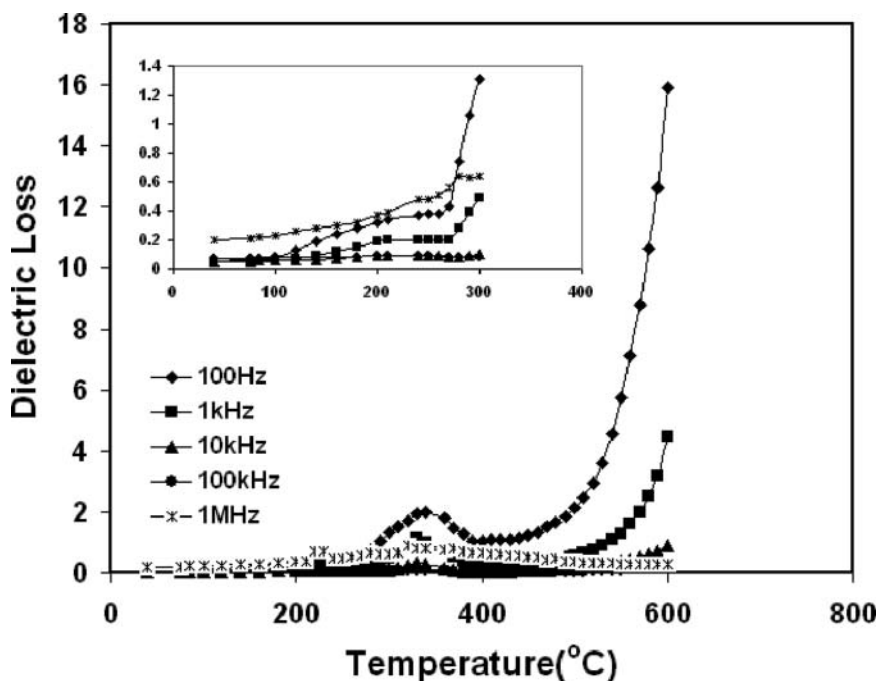


**Figure 11.** Temperature-dependence of dielectric loss of  $(1-x)(\text{Na}_{0.5}\text{Bi}_{0.5})\text{TiO}_3-x\text{Al}_6\text{Bi}_2\text{O}_{12}$  ( $x = 0.01$ ) at different frequencies before poling (lines for guiding the eyes only).

$(1-x)(\text{Na}_{0.5}\text{Bi}_{0.5})\text{TiO}_3-x\text{Al}_6\text{Bi}_2\text{O}_{12}$  with  $x = 0.03$  exhibits a large dielectric loss before transition temperature and it implies that poling will increase the movement of mobile ions. Fig. 10, shows the concentration  $x$ -dependence of the dielectric loss of  $(1-x)(\text{Na}_{0.5}\text{Bi}_{0.5})\text{TiO}_3-x\text{Al}_6\text{Bi}_2\text{O}_{12}$  ( $x = 0.01, 0.02, \text{ and } 0.03$ ) poled and unpoled at  $75^\circ\text{C}$  and  $100\text{Hz}$ . For the samples with  $x = 0.01$  and  $0.03$  seem to have lower dielectric loss and poling increases the dielectric loss. For the sample with  $x = 0.02$ , the dielectric loss seems enlarged, but poling reduces the dielectric loss.

Figures 11 and 12 show the temperature-dependence of dielectric loss of  $(1-x)(\text{Na}_{0.5}\text{Bi}_{0.5})\text{TiO}_3-x\text{Al}_6\text{Bi}_2\text{O}_{12}$  ( $x = 0.01$ ) at various frequencies in the temperature range  $45^\circ\text{C}$ – $600^\circ\text{C}$  for poled and unpoled samples. As is shown that dielectric loss increases with lowering frequency. It also can be seen that poled samples exhibit a larger dielectric loss than unpoled ones at low temperature. Large dielectric loss is mainly associated with the extrinsic factor such as mobile ions on the domain boundary. Our results indicate that poling will increase the movement of these mobile ions.

Figures 13 and 14 show polarization-electric field curve of  $(1-x)(\text{Na}_{0.5}\text{Bi}_{0.5})\text{TiO}_3-x\text{Al}_6\text{Bi}_2\text{O}_{12}$  ( $x = 0.01, 0.02 \text{ and } 0.03$ ) at room temperature for unpoled and poled samples respectively. From these two figures, it is shown that all of the samples exhibits well developed polarization electric field hysteresis loops, but the shapes of the hysteresis loops change with  $x$  very significantly. Figures 15–17 demonstrate concentration of  $\text{Al}_6\text{Bi}_2\text{O}_{12}$   $x$ -dependences of saturation polarization, remnant polarization and coercive field for unpoled and poled samples, respectively. From Figs. 15 and 16, it can be seen that poled samples exhibit a larger saturation polarization and remnant polarization. The saturate and remnant polarization seems to reach the optimum  $16.90\mu\text{C}/\text{cm}^2$  and  $10.66\mu\text{C}/\text{cm}^2$  respectively,

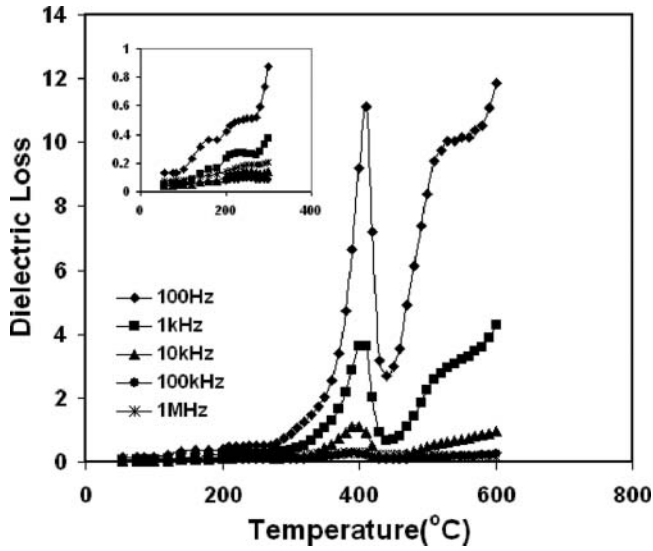


**Figure 12.** Temperature-dependence of dielectric loss of  $(1-x)(\text{Na}_{0.5}\text{Bi}_{0.5})\text{TiO}_3-x\text{Al}_6\text{Bi}_2\text{O}_{12}$  ( $x = 0.01$ ) at different frequencies after poling (lines for guiding the eyes only).

when  $x = 0.02$ . For poled samples with  $x = 0.02$ , they are  $20.41\ \mu\text{C}/\text{cm}^2$  and  $15.05\ \mu\text{C}/\text{cm}^2$ , respectively. From Fig. 17, for unpoled samples, the coercive field decreases with increasing  $x$ . For poled samples, the lower coercive field  $E_c$  appears at  $x = 0.02$ . The decrease in the  $E_c$  is associated with random field around dipolar defects which lower the activation barrier required for the nucleation of domains [22]. The increase of the coercive field with the increasing  $x$  from 0.02 to 0.03 for poled sample could be possibly explained by the reason

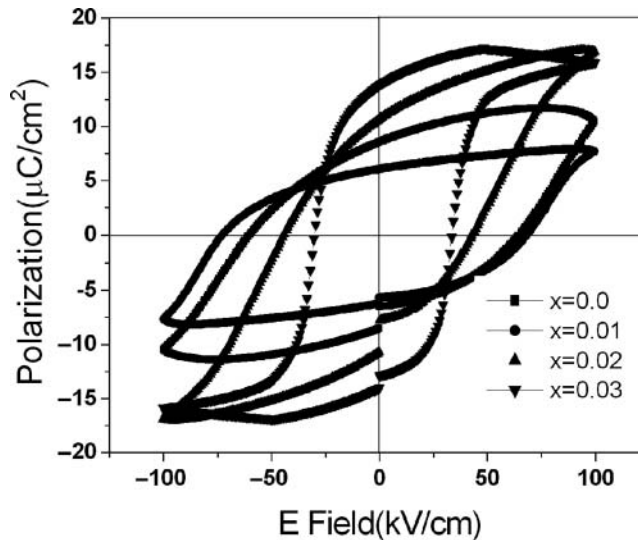


**Figure 13.** Ferroelectric hysteresis of  $(1-x)(\text{Na}_{0.5}\text{Bi}_{0.5})\text{TiO}_3-x\text{Al}_6\text{Bi}_2\text{O}_{12}$  ( $x = 0.01, 0.02$  and  $0.03$ ) at room temperature before poling.

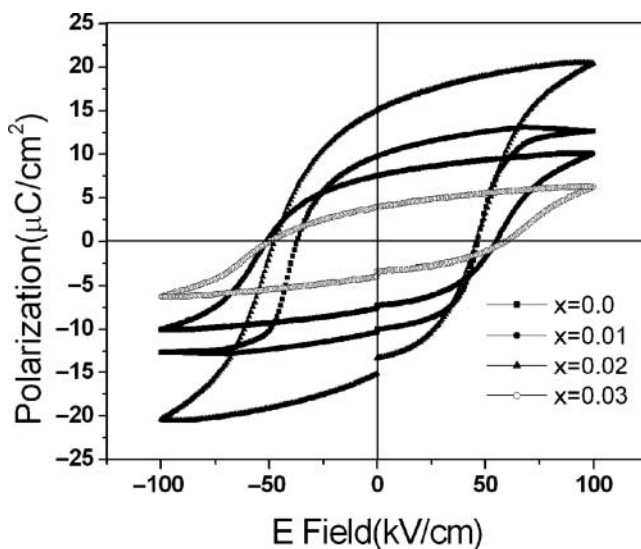


**Figure 14.** Ferroelectric hysteresis of  $(1-x)(\text{Na}_{0.5}\text{Bi}_{0.5})\text{TiO}_3-x\text{Al}_6\text{Bi}_2\text{O}_{12}$  ( $x = 0.0, 0.01, 0.02,$  and  $0.03$ ) at room temperature after poling.

that poling increases the movement of mobile ions and affects the combination of oxygen vacancies with  $\text{Al}^{3+}$  ions on the B site. This leads to the reduction of chance for formation of dipolar defects.

Figures 18 and 19 show the response of strain to the electric field for unpoled and poled sample of  $(1-x)(\text{Na}_{0.5}\text{Bi}_{0.5})\text{TiO}_3-x\text{Al}_6\text{Bi}_2\text{O}_{12}$  ( $x = 0.02$ ) respectively. It is clearly shown in

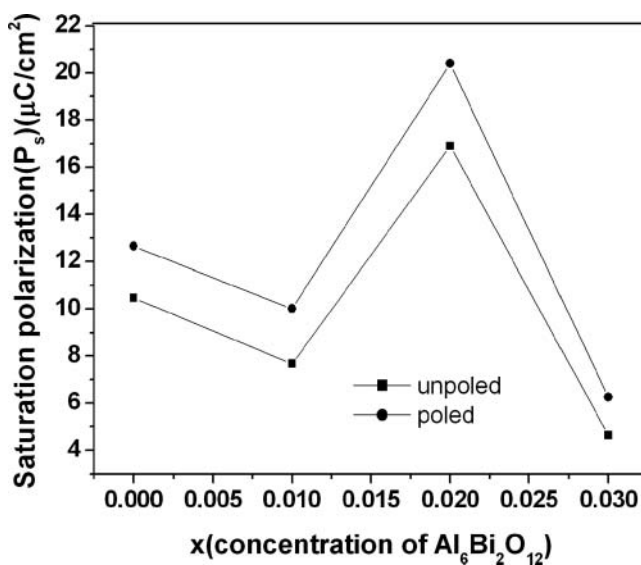


**Figure 15.** Concentration dependence of saturation polarization of  $(1-x)(\text{Na}_{0.5}\text{Bi}_{0.5})\text{TiO}_3-x\text{Al}_6\text{Bi}_2\text{O}_{12}$  At room temperature (lines for guiding the eyes only).

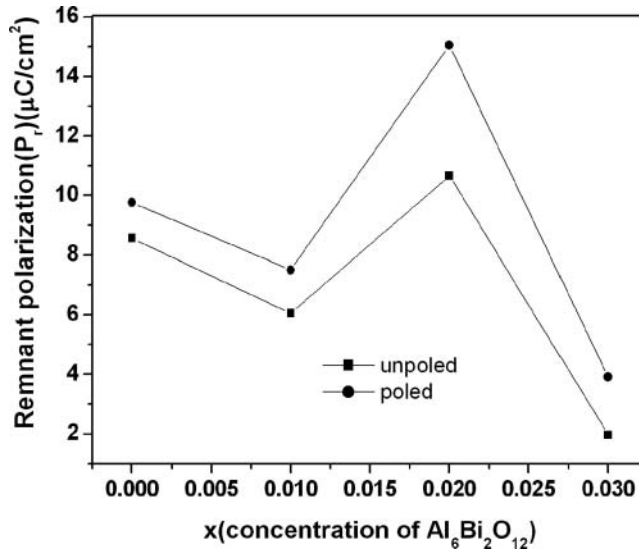


**Figure 16.** Concentration  $x$ -dependence of remnant polarization of  $(1-x)(\text{Na}_{0.5}\text{Bi}_{0.5})\text{TiO}_3-x\text{Al}_6\text{Bi}_2\text{O}_{12}$  at room temperature (lines for guiding the eyes only).

Fig. 18 that  $(1-x)\text{NBT}-x\text{Al}_6\text{Bi}_2\text{O}_{12}$  ( $x = 0.02$ ) is a typical electrostrictive material before poling and it is shown in Fig. 19 that it has a strong piezoelectric behavior after poling. The piezoelectric constant  $d_{33}$  increases from  $20\text{pC/N}$  for unpoled sample to  $400\text{pC/N}$  for poled one with  $x = 0.02$ . NBT- $\text{Al}_6\text{Bi}_2\text{O}_{12}$  ceramics exhibit improved piezoelectric properties compared with the pure NBT and NBT- $\text{BiAlO}_3$  [20]. The piezoelectric constant  $d_{33}$  of the

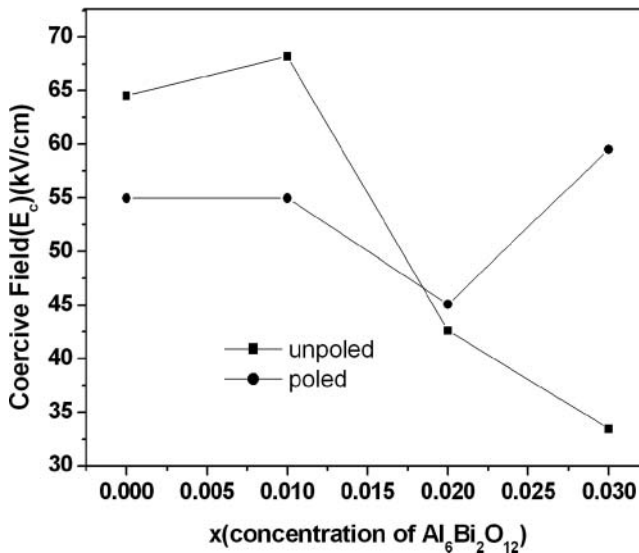


**Figure 17.** Concentration  $x$ -dependence of coercive field of  $(1-x)(\text{Na}_{0.5}\text{Bi}_{0.5})\text{TiO}_3-x\text{Al}_6\text{Bi}_2\text{O}_{12}$  At room temperature (lines for guiding the eyes only).

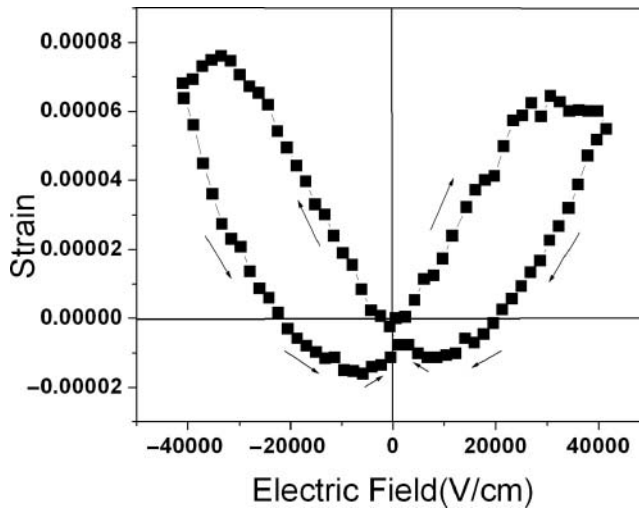


**Figure 18.** Strain vs. applied electric field for  $(1-x)(\text{Na}_{0.5}\text{Bi}_{0.5})\text{TiO}_3\text{-}x\text{Al}_6\text{Bi}_2\text{O}_{12}$  ( $x = 0.02$ ) at room temperature before poling. (lines for guiding the eyes only).

pure NBT ceramics has been investigated and it is reported to be  $77\text{pC/N}$  [22] for poled samples. Our results is as high as  $400\text{pC/N}$  for poled  $(1-x)\text{NBT-}x\text{Al}_6\text{Bi}_2\text{O}_{12}$  with  $x = 0.02$ . Figure 20 shows  $d_{33}$  of poled  $(1-x)\text{NBT-}x\text{Al}_6\text{Bi}_2\text{O}_{12}$  ( $x = 0.01, 0.02, 0.03$ ) samples. From this figure, it can be seen that piezoelectric constant  $d_{33}$  decreases with increasing concentration of  $\text{Al}_6\text{Bi}_2\text{O}_{12}$   $x$ . The improved piezoelectric properties are believed to be associated with the decreased conductivity. Figure 20 indicates the addition of  $\text{Al}_6\text{Bi}_2\text{O}_{12}$  will increase mobility of ions which, in turn, causes the increase of energy loss. It is a setback. There is work to do to overcome this problem.

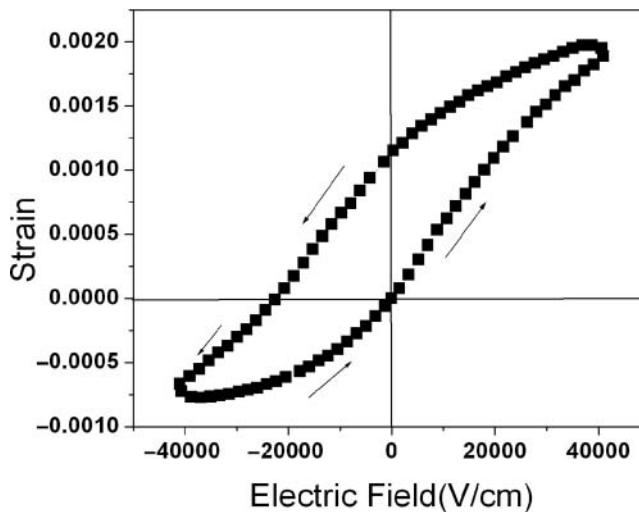


**Figure 19.** Strain vs. applied electric field for  $(1-x)(\text{Na}_{0.5}\text{Bi}_{0.5})\text{TiO}_3\text{-}x\text{Al}_6\text{Bi}_2\text{O}_{12}$  ( $x = 0.02$ ) at room temperature after poling. (lines for guiding the eyes only).

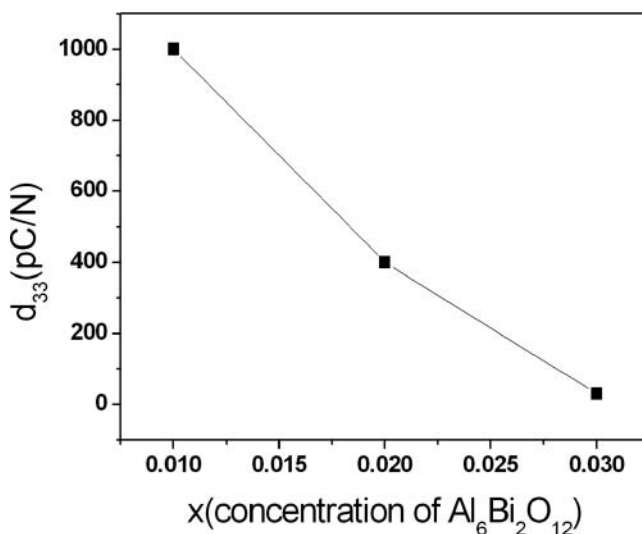


**Figure 20.** Concentration  $x$ -dependence of  $d_{33}$  of  $(1-x)(\text{Na}_{0.5}\text{Bi}_{0.5})\text{TiO}_3-x\text{Al}_6\text{Bi}_2\text{O}_{12}$  for poled samples (lines for guiding the eyes only).

#### 4. Conclusions

$(1-x)(\text{Na}_{0.5}\text{Bi}_{0.5})\text{TiO}_3-x\text{Al}_6\text{Bi}_2\text{O}_{12}$  with  $x = 0.01, 0.02, 0.03$  has been synthesized by conventional solid-state reaction sintering method.  $(\text{Na}_{0.5}\text{Bi}_{0.5})\text{TiO}_3-\text{Al}_6\text{Bi}_2\text{O}_{12}$  solid solution exhibit improved ferroelectric and piezoelectric properties compared with the NBT-BiAlO<sub>3</sub> solid solution. The poled  $(1-x)(\text{Na}_{0.5}\text{Bi}_{0.5})\text{TiO}_3-x\text{Al}_6\text{Bi}_2\text{O}_{12}$  with  $x = 0.01, 0.02, 0.03$  demonstrate higher remnant polarization but lower coercive field compared with samples before poling. Certain amount of addition of  $\text{Al}_6\text{Bi}_2\text{O}_{12}$  will enhance the performance of  $(\text{Na}_{0.5}\text{Bi}_{0.5})\text{TiO}_3$  and poling will improve the dielectric and piezoelectric properties of ceramics. However, poling may increase the dielectric loss and the improvement is needed in this regard.

#### Acknowledgments

This work is supported by the Office of Naval Research, US Navy, Grant N00014-08-1-0785.

#### References

1. J. Rödel, W. Jo, K. T. P. Seifert, E.-M. Anton, and T. Granzow, Perspective on the development of lead-free piezoceramics. *J. Am. Ceram. Soc.* **92**(25), 1153–1177 (2009).
2. R. Guo, L. E. Cross, S.-E. Park, B. Noheda, D. E. Cox, and G. Shirane, Origin of the high piezoelectric response in  $\text{PbZr}_{1-x}\text{Ti}_x\text{O}_3$ . *Phys. Rev. Lett.* **84**(4), 5423–5426 (2000).
3. G. A. Smolenskii, V. A. Isupov, A. I. Afraonovskaya, and N. N. Krainik, New ferroelectrics of complex composition IV. *Sov. Phys. Solid State* **2**(4), 2651–2654 (1961).
4. D. Z. Jin, X. M. Chen, and Z. C. Xu, Influence of dispersed coarse grains on mechanical and piezoelectric properties in  $(\text{Bi}_{1/2}\text{Na}_{1/2})\text{TiO}_3$  ceramics. *Mater. Lett.* **58**(5), 1701–1705 (2004).
5. T. Takenaka, K. Sakata, and K. Toda, Piezoelectric. Properties of  $(\text{Bi}_{1/2}\text{Na}_{1/2})\text{TiO}_3$ -based ceramics. *Ferroelectrics* **106**(6), 375–380 (1990).

6. H. Nagata and T. Takenaka, Additive effects on electrical properties of  $(\text{Bi}_{1/2}\text{Na}_{1/2})\text{TiO}_3$  ferroelectric ceramics. *J. Eur. Ceram. Soc.* **21**(4), 1299–1302 (2001).
7. S. Niitaka, M. Azuma, M. Takano, E. Nishibori, M. Takata, and M. Sakata, Crystal structure and dielectric and magnetic properties of  $\text{BiCrO}_3$  as a ferroelectromagnet. *Solid State Ionics* **172**(3), 557–559 (2004).
8. F. Sugawara, S. Iida, Y. Syono, and S. Akimoto, Magnetic properties and crystal distortions of  $\text{BiMnO}_3$  and  $\text{BiCrO}_3$ . *J. Phys. Soc. Japan* **25**(6), 1553–1558 (1968).
9. A. A. Belik, S. Iikubo, K. Kodama, N. Igawa, S.-I. Shamoto, S. Niitaka, M. Azuma, Y. Shimakawa, M. Takano, F. Izumi, and E. T. Muromachi, Neutron powder diffraction study on the crystal and magnetic structures of  $\text{BiCoO}_3$ . *Chem. Mater.* **18**(6), 798–803 (2006).
10. S. Ishiwata, M. Azuma, M. Takano, E. Nishibori, M. Takata, M. Sakata, and K. Kato, High pressure synthesis, crystal structure and physical properties of a new Ni(II) perovskite  $\text{BiNiO}_3$ . *J. Mater. Chem.* **12**(5), 3733–3737 (2002).
11. M. V. Madhava Rao and Chen-Feng Kao,  $(\text{Bi}_{0.5}\text{Na}_{0.5})_{0.93}\text{Ba}_{0.07}\text{TiO}_3$  lead-free ceramics with addition of  $\text{Ga}_2\text{O}_3$ . *Physica B* **403**(3), 3596–3598 (2008).
12. Y. M. Chiang, G. W. Farrey, and A. N. Soukhovjak, Lead-free high-strain single-crystal piezoelectrics in the alkaline–bismuth–titanate perovskite family. *Appl. Phys. Lett.* **73**(3), 3683–3685 (1998).
13. T. Wada, K. Toyoiike, Y. Imanaka, and Y. Matsuo, Dielectric and piezoelectric properties of  $(\text{A}_{0.5}\text{Bi}_{0.5})\text{TiO}_3\text{-ANbO}_3$  ( $\text{A} = \text{Na}, \text{K}$ ) systems. *Jpn. J. Appl. Phys.* **40**(3), 5703–5705 (2001).
14. H. Ishii, H. Nagata, and T. Takenaka, Morphotropic phase boundary and electrical properties of bismuth sodium titanate—potassium niobate solid-solution ceramics. *Jpn. J. Appl. Phys.* **40**(4), 5660–5663 (2001).
15. J.-R. Gomah-Petry, S. Said, P. Marchet, and J.-P. Mercurio, Sodium-bismuth titanate based lead-free ferroelectric materials. *J. Eur. Ceram. Soc.* **24**(5), 1165–1169 (2004).
16. P. Marchet, E. Boucher, V. Dorcet, and J. P. Mercurio, Dielectric properties of some low-lead or lead-free perovskite-derived materials:  $\text{Na}_{0.5}\text{Bi}_{0.5}\text{TiO}_3\text{-PbZrO}_3$ ,  $\text{Na}_{0.5}\text{Bi}_{0.5}\text{TiO}_3\text{-BiScO}_3$  and  $\text{Na}_{0.5}\text{Bi}_{0.5}\text{TiO}_3\text{-BiFeO}_3$  ceramics. *J. Eur. Ceram. Soc.* **26**(5), 3037–3041 (2006).
17. J. Wang, J. B. Neaton, H. Zheng, V. Nagarajan, S. B. Ogale, B. Liu, D. Viehland, V. Vaithyanathan, D. G. Schlom, U. V. Waghmare, N. A. Spaldin, K. M. Rabe, M. Wuttig, and R. Ramesh, Epitaxial  $\text{BiFeO}_3$  multiferroic thin film heterostructures. *Science* **299**(4), 1719–1722 (2003).
18. P. Baettig, C. F. Schelle, R. LeSar, U. V. Waghmare, and N. A. Spaldin, Theoretical prediction of new high-performance lead-free piezoelectrics. *Chem. Mater.* **17**(5), 1376–1380 (2005).
19. A. A. Belik, T. Wuernisha, T. Kamiyama, K. Mori, M. Maie, T. Nagai, Y. Matsui, and E. Takayama-Muromachi, High-pressure synthesis, crystal structures, and properties of perovskite-like  $\text{BiAlO}_3$  and pyroxene-like  $\text{BiGaO}_3$ . *Chem. Mater.* **18**(7), 133–139 (2006).
20. Huichun Yu and Zuo-Guang Ye, Dielectric, ferroelectric, and piezoelectric properties of the lead-free  $(1-x)(\text{Na}_{0.5}\text{Bi}_{0.5})\text{TiO}_3\text{-}x\text{BiAlO}_3$  solid solution. *Appl. Phys. Lett.* **93**(3), 112902–112904 (2008).
21. Huichun Yu and Zuo-Guang Ye, Dielectric properties and relaxor behavior of a new  $(1-x)\text{BaTiO}_3\text{-}x\text{BiAlO}_3$  solid solution. *J. Appl. Phys.* **103**(5), 034114–034118 (2008).
22. D. Viehland and Y. H. Chen, Random-field model for ferroelectric domain dynamics and polarization reversal. *J. Appl. Phys.* **88**(12), 6696–6707 (2000).
23. J. H. Park, B. K. Kim, and S. J. Park, Electrostrictive coefficients of  $0.9\text{Pb}(\text{Mg}_{1/3}\text{Nb}_{2/3})\text{O}_3\text{-}0.1\text{PbTiO}_3$  relaxor ferroelectric ceramics in the ferroelectricity-dominated temperature range. *J. Am. Ceram. Soc.* **79**(5), 430–434 (1996).
24. S. E. Park and K. S. Hong, Variations of structure and dielectric properties on substituting A-site cations for  $\text{Sr}^{2+}$  in  $(\text{Na}_{1/2}\text{Bi}_{1/2})\text{TiO}_3$ . *J. Mater. Res.* **12**(6), 2152–2157 (1997).